A Novel Co-ordination Mode for the Squarate Ligand [Dihydroxycyclobutenedionate(2−)]: Synthesis, Crystal Structure, and Magnetic Properties of *catena*-Diaqua(2,2′-bipyridyl)-μ-(squarato-O^1,O^2)-nickel(II) Dihydrate†

Régis Soules, Françoise Dahan, Jean-Pierre Laurent, and Paule Castan *
Laboratoire de Chimie de Coordination du CNRS, Unité no. 8241 liée par convention à l'Université Paul Sabatier, 205 route de Narbonne, 31077 Toulouse Cedex, France

The crystal and molecular structure of *catena*-diaqua(2,2′-bipyridyl)-μ-(squarato-O^1,O^2)-nickel(II) dihydrate, $[\{Ni(C_4O_4)(C_{10}H_8N_2)(H_2O)_2{\cdot}2H_2O\}_n]$ [squarate = dihydroxycyclobutenedionate(2−)] has been determined by single-crystal *X*-ray analysis. The compound crystallizes in the monoclinic system, space group $P2_1/c$, with a = 11.724(2), b = 7.418(1), c = 19.343(3) Å, and β = 100.16(2)°. The crystal structure contains chains of squarato-O^1,O^2-bridged Ni^{II} metal atoms. These chains are held together by strong hydrogen bonds between the non-co-ordinating oxygen atoms of the squarate anions and the water molecules. Variable-temperature (4.2—290 K) magnetic susceptibilities were determined; the squarato-O^1,O^2 bridge cannot mediate in a significant exchange interaction.

Interactions between paramagnetic metal ions in coupled systems have been a subject of interest for a number of years, in view of evidence of antiferromagnetic exchange as well as ferromagnetic interactions. One of the most interesting themes developed was the study of strong interactions through extended bridging ligands between metal ions far away from each other.[1-3] Oxalate-bridged dimers have been known for some time and in previous work it has been observed that the squarate(2−) ion [dihydroxycyclobutenedionate(2−)] can exhibit a number of co-ordination possibilities, making it a particularly interesting potential ligand.[2-8]

The impetus for the choice of complexes of nickel squarate was their co-ordination polymer structure and the possibility of the squarate ion π-electron system acting as a path for magnetic superexchange between metal ions. With this in mind, two complexes involving nickel and squaric acid, nickel squarate, $[\{Ni(C_4O_4){\cdot}2H_2O\}_n]$,[5] and *catena*-diaquabis(imidazole)-μ-(squarato-O^1,O^3)-nickel(II), $[\{Ni(C_4O_4)(C_3H_4N_2)_2(H_2O)_2\}_n]$,[4] have already been investigated by both *X*-ray crystal structure determination and magnetic studies. The co-ordination pattern of the squarate ion is largely different in these two complexes. In the former, each squarate oxygen is bound to a different nickel atom forming a sheet structure, whereas in the latter, two of the oxygen atoms, namely the diagonally positioned O(1) and O(3), co-ordinate directly to nickel atoms to yield a chain structure through squarato-O^1,O^3 bridges. A third co-ordination mode involving a bis-chelating (1,2 and 3,4) squarate anion has been assumed in the case of a dinuclear nickel complex.[9] To our knowledge, this possibility, which would parallel the bis-chelating behaviour of the oxalate anion, has not yet been supported by any structural determination. Considering the steric requirements of the squarate anion casts some doubt upon such a co-ordination mode, *i.e.* chelation through adjacent oxygen atoms. However, 1,2-chelation has been observed in the case of the dithiosquarate anion.[10,11]

We present here the *X*-ray crystal structure and magnetic properties of a novel complex prepared from Ni^{II} and squaric acid, in which the squarate anion exhibits complexing behaviour of a type not previously described, *i.e.* formation of a chain structure through squarato-O^1,O^2 bridges.

† *Supplementary data available:* see Instructions for Authors, *J. Chem. Soc., Dalton Trans.*, 1988, Issue 1, pp. xvii—xx.
Non-S.I. unit employed: $\chi_{c.g.s} = \chi_{S.I.} \times 10^6/4\pi$.

Experimental

Synthesis.—Transparent blue crystals of $[\{Ni(C_4O_4)(C_{10}H_8N_2)(H_2O)_2{\cdot}2H_2O\}_n]$ were slowly grown from a mixture of $NiCl_2{\cdot}6H_2O$ in water (10 cm^3, 0.01 mol dm^{-3}), $H_2C_4O_4$ in water (10 cm^3, 0.01 mol dm^{-3}), and 2,2′-bipyridine in water (10 cm^3, 0.01 mol dm^{-3}). The solution rapidly turned mauve in colour, then became blue. After 2 h a blue precipitate appeared which was filtered off. From the resulting solution, blue needles could be isolated (Found: C, 42.10; H, 4.00; N, 7.15; Ni, 14.20. Calc. for $C_{14}H_{16}N_2NiO_8$: C, 42.15; H, 4.00; N, 7.00; Ni, 14.70%). The same analysis was found for the precipitate as for the blue needles. The total yield was 90%.

Physical Measurements.—Routine i.r. spectra were recorded on a Perkin-Elmer 577 spectrophotometer using KBr pellets. Powder reflectance spectra were obtained with a Cary 21 G spectrophotometer using an integration sphere at room temperature.

Magnetic susceptibility data were collected on powdered samples of the compounds using a Faraday-type magnetometer with mercury tetrakis(thiocyanato)cobaltate (susceptibility at 20 °C, 16.44 × 10^{-6} cm^3 mol^{-1}) as the susceptibility standard. Data were corrected for diamagnetism of the ligands and anions (estimated from Pascal constants to be −1.3 × 10^{-4} cm^3 mol^{-1}) and for temperature-independent paramagnetism (t.i.p.). This latter term was estimated to be 200 × 10^{-6} cm^3 mol^{-1}. E.s.r. spectra were recorded at *X*-band frequency (9.4—9.5 GHz) with a Bruker 200 TT-spectrometer.

X-*Ray Crystallography.*—*Crystal data.* $C_{14}H_{16}N_2NiO_8$, M = 399.0, monoclinic, space group $P2_1/c$ (C_{2h}, no. 14), a = 11.724(2), b = 7.418(1), c = 19.343(3) Å, β = 100.16(2)°, U = 1 655.9 $Å^3$, Z = 4, D_c = 1.60 g cm^{-3}, $F(000)$ = 824, Mo-K_α radiation, λ = 0.710 73 Å, μ = 12.2 cm^{-1}, 293 K.

Data collection. A blue needle-like crystal of dimensions 0.162 (010, 010) × 0.050 (101, 101) × 0.025 (101, 101) mm (distances from centre to faces) was centred on an Enraf-Nonius CAD4 diffractometer equipped with a graphite monochromator. The unit-cell dimensions were determined from the setting angles of 25 reflections in the range 8.5 < θ < 12.5°. A data set of 4 691 reflections (1.5 < θ < 28.5°; $h, k, \pm l$) was recorded as described peviously[12] by the θ–2θ scan technique (scan width 0.80 + 0.35 tan θ, scan speed 1.1—10.1° min^{-1}). The intensities of three standard reflections monitored every 2 h showed no

Table 1. Fractional atomic co-ordinates with estimated standard deviations (e.s.d.s) in parentheses

Atom	*x*	*y*	*z*	Atom	*x*	*y*	*z*
Ni	0.258 90(4)	0.169 53(8)	0.620 77(2)	C(14)	0.211 4(4)	−0.232 7(5)	0.580 9(2)
N(1)	0.320 1(3)	0.171 2(5)	0.727 8(2)	O(3)	0.113 4(3)	0.453 1(4)	0.463 2(2)
C(1)	0.437 2(3)	0.162 3(6)	0.745 6(2)	O(4)	0.098 2(3)	−0.116 3(4)	0.467 9(2)
C(2)	0.490 8(4)	0.154 5(8)	0.815 7(2)	O(W1)	0.221 7(3)	0.165 2(4)	0.514 2(1)
C(3)	0.423 7(5)	0.158 2(9)	0.867 1(2)	O(W2)	0.088 7(2)	0.172 1(5)	0.633 6(2)
C(4)	0.305 6(5)	0.168 5(8)	0.849 0(2)	O(W3)	0.008 6(3)	0.519 7(5)	0.327 0(2)
C(5)	0.257 5(4)	0.175 8(7)	0.779 0(2)	O(W4)	0.103 3(4)	0.718 7(6)	0.227 7(2)
N(2)	0.435 4(3)	0.164 9(5)	0.622 8(2)	H(11)	0.194(4)	0.278(4)	0.492(2)
C(6)	0.501 8(3)	0.163 0(6)	0.687 1(2)	H(12)	0.168(4)	0.076(5)	0.490(2)
C(7)	0.621 3(4)	0.157 8(8)	0.695 9(3)	H(21)	0.029(3)	0.156(7)	0.592(2)
C(8)	0.673 7(4)	0.162 2(9)	0.637 9(3)	H(22)	0.064(4)	0.281(4)	0.654(3)
C(9)	0.606 1(5)	0.162 7(9)	0.572 5(3)	H(31)	0.044(4)	0.488(8)	0.375(1)
C(10)	0.487 5(4)	0.168 6(7)	0.566 7(2)	H(32)	−0.025(4)	0.405(4)	0.310(3)
O(1)	0.254 1(3)	−0.116 3(3)	0.625 4(2)	H(41)*	0.058(4)	0.656(6)	0.259(2)
O(2)	0.261 4(3)	0.453 2(3)	0.623 4(2)	H(42)*	0.141(4)	0.632(6)	0.201(2)
C(11)	0.216 7(4)	0.569 3(5)	0.580 3(2)	H(43)*	0.034(4)	0.668(6)	0.199(2)
C(12)	0.148 4(4)	0.570 2(6)	0.509 2(2)	H(44)*	0.110(4)	0.648(6)	0.271(2)
C(13)	0.142 4(3)	−0.234 9(5)	0.510 7(2)				

* Occupancy factor equal to 0.5.

significant variation during data collection. After rejection of systematic absences ($h0l$, $l \neq 2n$ and $0k0$, $k \neq 2n$), 4 366 reflections were corrected for Lorentz and polarization effects,[13] 2 174 with $I > 3\sigma(I)$ being considered 'observed' and corrected for absorption[14] (max., min. transmission factors 0.94, 0.76). After averaging of $0kl$ and $0k\bar{l}$ reflections ($R_{av.} = 0.022$), 2 075 independent reflections were used for the structure solution and least-squares refinement.

Structure determination. The structure was solved by the heavy-atom method. After location of the Ni atom by a Patterson map, subsequent full-matrix least-squares refinement and interpretation of Fourier difference maps using SHELX[15] enabled all non-hydrogen atoms in the structure to be located, with two unexpected water molecules; these were refined anisotropically. Hydrogen atoms were located on a Fourier difference map. Those of the bipyridine ring were introduced into the calculations with a constrained geometry (C–H = 0.97 Å) and fixed isotropic thermal parameters, $U = 0.05$ Å^2. Hydrogens of the O(W4) water molecule appeared to be disordered. They were introduced in four positions with an occupancy factor of 50%. Common isotropic thermal parameters were assigned to hydrogens bonded to O(W1) and O(W2) on the one hand, and to those bonded to O(W3) and O(W4) on the other, and allowed to vary. The O(W)–H bond lengths, at first constrained to 0.97 Å, were unconstrained in the last cycle of refinement. Neutral atom scattering factors were used, those for non-hydrogen atoms being corrected for anomalous dispersion (f', f'').[16] Weights, $w = [\sigma^2(F_o) + (0.035\,F_o)^2]^{-1}$, were applied and gave satisfactory weight analysis. In the last full-matrix least-squares refinement cycle no shifts were greater than 0.05 times the estimated standard deviation for non-hydrogen atom parameters and the final R was 0.036 ($R' = 0.048$). A final Fourier difference map showed no excursion of electron density greater than 0.4 e Å^{-3}. All calculations were performed on a VAX-11/730 DEC computer. Atomic co-ordinates are listed in Table 1.

Additional material available from the Cambridge Crystallographic Data Centre comprises H-atom co-ordinates, thermal parameters, remaining bond lengths and angles, and hydrogen bonding interactions.

Results and Discussion

Description and Discussion of the Crystal Structure.—The ORTEP plot of the molecule along with the labelling scheme is shown in Figure 1. Selected interatomic bond distances and angles are reported in Table 2.

Table 2. Selected bond lengths (Å) and angles (°) with e.s.d.s in parentheses

Nickel environment			
Ni–N(1)	2.069(3)	Ni–O(2)	2.105(3)
Ni–N(2)	2.063(3)	Ni–O(W1)	2.030(3)
Ni–O(1)	2.124(3)	Ni–O(W2)	2.054(3)
N(1)–Ni–N(2)	79.1(1)	N(2)–Ni–O(W2)	172.1(1)
N(1)–Ni–O(1)	88.3(1)	O(1)–Ni–O(2)	176.0(1)
N(1)–Ni–O(2)	88.2(1)	O(1)–Ni–O(W1)	91.4(1)
N(1)–Ni–O(W1)	172.2(1)	O(1)–Ni–O(W2)	88.3(1)
N(1)–Ni–O(W2)	93.0(1)	O(2)–Ni–O(W1)	92.3(1)
N(2)–Ni–O(1)	90.9(1)	O(2)–Ni–O(W2)	89.9(1)
N(2)–Ni–O(2)	90.4(1)	O(1)–Ni–O(W2)	94.8(1)
N(2)–Ni–O(W1)	90.4(1)		
Squarate environment			
C(11)–C(12)	1.465(6)	C(11)–O(2)	1.249(5)
C(12)–C(13^i)	1.448(6)	C(12)–O(3)	1.259(5)
C(13)–C(14)	1.454(6)	C(13^i)–O(4^i)	1.255(5)
C(14^i)–C(11)	1.471(6)	C(14^i)–O(1^i)	1.258(5)
Ni–O(1)–C(14)	131.8(3)	Ni–O(2)–C(11)	132.1(3)
C(12)–C(11)–C(14^i)	89.2(3)	C(11)–C(12)–C(13^i)	90.4(3)
C(12)–C(11)–O(2)	136.6(4)	C(11)–C(12)–O(3)	135.7(4)
O(2)–C(11)–C(14^i)	134.2(4)	O(3)–C(12)–C(13^i)	133.8(4)
C(12)–C(13^i)–C(14^i)	90.5(3)	C(11)–C(14^i)–C(13^i)	89.9(3)
C(12)–C(13^i)–O(4^i)	134.6(4)	C(11)–C(14^i)–O(1^i)	132.7(4)
O(4^i)–C(13^i)–C(14^i)	134.8(4)	O(1^i)–C(14^i)–C(13^i)	137.3(4)

Symmetry operation i: x, $1 + y$, z.

Figure 1 shows that the crystal structure of the complex consists of chains built up of squarato-O^1,O^2-bridged nickel(II) ions. In contrast to the zig-zag chain observed in $[\{Ni(C_4O_4)(C_3H_4N_2)_2(H_2O)_2\}_n]$, which results from 1,3-co-ordination of the bridging anion, 1,2-co-ordination leads to a perfectly linear chain running parallel to the b axis (see Figure 2). Within each chain, each metal atom is octahedrally co-ordinated.

The four equatorial donor atoms, *i.e.* two nitrogen atoms from 2,2′-bipyridine and two oxygen atoms from two water molecules, are coplanar. The nickel atom is slightly displaced (*ca.* 0.009 Å) toward one axial oxygen, namely O(2), which

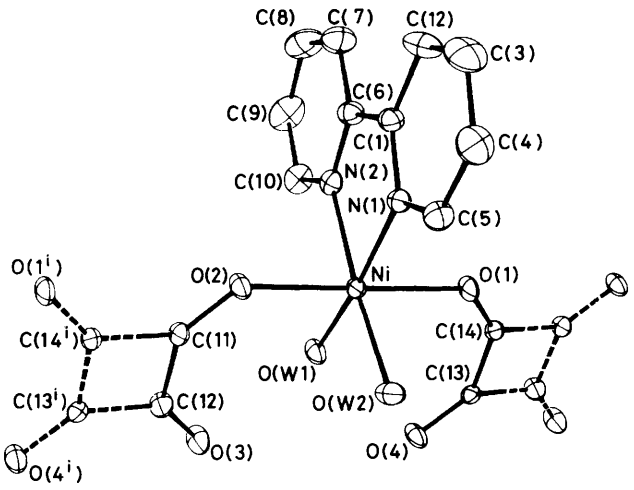

Figure 1. ORTEP plot of the $[Ni(C_4O_4)(C_{10}H_8N_2)(H_2O)_2]$ molecule with the labelling scheme. Hydrogen atoms are omitted for clarity

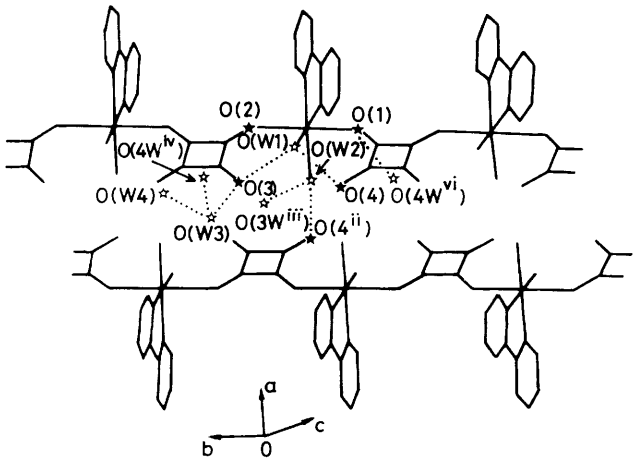

Figure 2. Molecular packing with a schematic representation of hydrogen bonds. Black stars represent squarate oxygen atoms and white stars water molecules

unlike the other axial donor, O(1), is not involved in hydrogen bonding. However these two oxygen atoms are symmetrically positioned with respect to the mean co-ordination plane. Interestingly, the axial bonds, Ni–O(1) and Ni–O(2), are bent away from the equatorial O(W1). Furthermore the two equatorial Ni–O(W) bonds have different lengths, Ni–O(W1) being 0.024(3) Å shorter than Ni–O(W2). These features are likely to be related to the fact that O(W1) is involved in two strong intramolecular hydrogen bonds (see below).

The squarate anion is planar within the limits of error. The C–C bond lengths [1.471(6), 1.465(6), 1.454(6), and 1.448(6) Å] are close to the values found in $[\{Ni(C_4O_4)(C_3H_4N_2)_2(H_2O)_2\}_n]$ [1.463(2) and 1.470(2) Å][4] or in the free acid [1.456(12) Å][17] but smaller than the value [1.487(16) Å] reported for $[\{Ni(C_4O_4)\cdot 2H_2O\}_n]$.[5] The O–C–C angles [132.7(4)—137.3(4)°] are similar to those reported for squaric acid, $[\{Ni(C_4O_4)(C_3H_4N_2)_2(H_2O)_2\}_n]$, and $[\{Ni(C_4O_4)\cdot 2H_2O\}_n]$. The C–C–C angles are very close to 90°. The internal geometry of the bipyridine ligand is normal and so will not be discussed further.

Of particular interest in the structure is the presence of an extended network of strong hydrogen bonds (Figure 2). The

Table 3. Distances (Å) and angles (°) in the interactions of the type D–H ··· A (D = donor, A = acceptor)

D	H	A	H ··· A	D ··· A	D–H ··· A
O(W1)	H(11)	O(3)	1.65(3)	2.589(4)	163(5)
	H(12)	O(4)	1.67(4)	2.608(4)	163(4)
O(W2)	H(21)	O(4^{ii})	1.75(3)	2.703(4)	167(3)
	H(22)	O(W3^{iii})	1.77(4)	2.723(5)	166(4)
O(W3)	H(31)	O(3)	1.78(2)	2.748(4)	175(5)
	H(32)	O(W4^{iv})	1.75(4)	2.708(5)	171(4)
O(W4)	H(41)	O(W3)	1.84(3)	2.803(6)	166(3)
	H(42)	O(1^{v})	2.14(3)	2.976(6)	142(3)
	H(44)	O(W3)	2.00(4)	2.803(6)	139(3)

Symmetry operations: ii $-x, -y, 1-z$; iii $-x, 1-y, 1-z$; iv $-x, -\frac{1}{2}+y, \frac{1}{2}-z$; v $x, \frac{1}{2}-y, -\frac{1}{2}+z$.

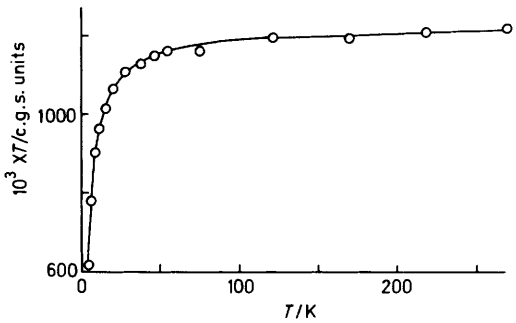

Figure 3. Plot of $\chi_M T$ *vs.* T. The line represents the theoretical values. Experimental values have been corrected for t.i.p. (200×10^{-6} cm^3 mol^{-1})

relevant data are reported in Table 3. As previously mentioned, one of the co-ordinated water molecules, namely O(W1), is hydrogen bonded to two unco-ordinated carbonyl oxygen atoms within the same mononuclear unit. The second co-ordinated water molecule, namely O(W2), is involved in inter-stack bonding to an unco-ordinated carbonyl oxygen atom and to the unco-ordinated water molecule O(W3). It can be emphasised that of the eight oxygen atoms present in the mononuclear unit only one, O(2), is not involved in hydrogen bonding.

Spectroscopic and Magnetic Data.—The infrared spectrum of the title complex displays two broad and intense bands located at 3 140 and 2 920 cm^{-1}. The observation of these low lying OH stretching vibrations agrees with the structural data pointing to the presence of strong hydrogen bonds. Bearing in mind the expression of Bellamy and Owen[18] which related the frequency of ν(OH) to the O ··· O distance of the hydrogen bridge, the bands at 3 140 and 2 920 cm^{-1} may be tentatively attributed to the OH group of the water molecule W(1) which is hydrogen bonded to O(3) and O(4) with small O–O distances of *ca.* 2.6 Å (*cf.* Table 3). Interpretation of the other part of the spectrum is not straightforward since, in the 1 550—1 450 cm^{-1} region for instance, several ill resolved absorptions overlap. These are attributable to the CO and CC stretching modes as well as numerous bipyridyl bands.

The u.v.–visible reflectance spectrum is dominated by a strong absorption at 235 nm with a shoulder at 330 nm. A band of low intensity is clearly observed at 610 nm while a fourth absorption is hardly discernible at *ca.* 870 nm. The band at 235

nm may be attributed to bipyridyl[19] whereas the bands at 610 and 870 nm are consistent with a quasi-octahedral geometry around the nickel ion. A more detailed assignment cannot be attempted due to the poor quality of the spectrum and to the fact that such an analysis would take into account not only the intrinsic low symmetry of the compound but also possible interactions between the ligand π orbitals and the filled and unfilled t_{2g} metal orbitals.

The $\chi_M T$ *vs.* temperature curve is reproduced in Figure 3. It can be seen that the χ_M values obey the Curie-Weiss law, $\chi_M = C/T - \theta$, yielding C and θ values of 1.23 and -3.53, respectively. The C value is within the range expected for an octahedrally co-ordinated nickel(II) ion, corresponding to a g value of 2.22. The negative value of θ suggests the occurrence of an antiferromagnetic interaction as does the attenuation of $\chi_M T$ at low temperatures. However, for nickel(II) complexes zero-field splitting cannot be excluded. The data available do not permit an estimation of the local anisotropy, more especially as very low temperature measurements are lacking. Tentatively, the data were fitted to an infinite isotropic Heisenberg chain model by using an analytical expression derived recently[20] from Weng's[21] results for an antiferromagnetic coupling ($J < 0$), *i.e.*: $\chi = N\beta^2 g^2/kT[(2 + 0.0194X + 0.777X^2)/(3 + 4.346X + 3.232X^2 + 5.834X^3)]$, with $X = |J|/kT$.

The least-squares fitting of the experimental data led to $g = 2.22$ and $J = -1.7$ cm^{-1}. In Figure 3, the best-fit curve is represented by a solid line and it can be seen that the fit to experimental data is good. Nevertheless the J value of -1.7 cm^{-1} has to be considered cautiously due to the neglect of additional interactions such as single-ion anisotropy, inter-chain exchange, and antisymmetric exchange.[22] Among these contributions, the most important would be likely to originate in the local anisotropy. Indeed, for a rather similar material containing chains of squarato-O^1,O^3-bridged nickel(II) ions, the magnetic data have been described by neglecting the influence of the exchange coupling, yielding a zero-field splitting parameter of $+5.8$ cm^{-1}.[4] All attempts to fit our data to the susceptibility expressions[23,24] for monomeric Ni^{II} with a zero-field splitting factor failed.

A more detailed analysis of the present data would require very low temperature experiments performed on a single crystal and/or heat capacity measurements.

Conclusions

Finally, the proper conclusion of the present study is that squarato-O^1,O^2 bridges behave very much like squarato-O^1,O^3 bridges in the sense that they cannot mediate significant exchange interaction. As previously suggested for a dinuclear nickel complex which has been shown to display a weak antiferromagnetic interaction ($J \sim 0.4$ cm^{-1}),[9] the failure of squarate anions to promote significant exchange interaction is likely to be related to stabilization of the ligand orbitals by the large π delocalization which characterizes the squarate ring.

In the present complex and in $[\{Ni(C_4O_4)(C_3H_4N_2)_2(H_2O)_2\}_n]$, the most probable exchange pathway is provided by the σ-orbital system and may involve d_{z^2}-like orbitals (the z axis being taken along the chain) on the nickel atoms and bridge orbitals built up from oxygen and carbon in-plane (p_z and p_y) orbitals. It would therefore be interesting to look at the possibility of the ligand π system participating in the exchange mechanism. Within the framework of a chain structure similar to that of the present complex, this would require that the unpaired electron orbitals would be of π symmetry and suitably orientated to overlap the ligand π-orbital system. From these requirements one may infer that the most suitable electronic configuration at the metal atoms would involve unpaired spin in the d_{xz} and/or d_{zy} orbitals as is the case for the Mn^{II} ion. In this instance, the exchange mechanism would be sensitive to rotation of the squarate plane around the z axis. The largest interactions would correspond to this plane being parallel either to the xz plane, with a d_{yz} unpaired electron, or to the yz plane with a d_{xz} unpaired electron.

Acknowledgements

We are grateful to a referee who drew our attention to the possibility of an exchange mechanism through the π system of the squarate anion.

References

1 C. Chauvel, J-J. Girerd, Y. Jeannin, O. Kahn, and G. Lavigne, *Inorg. Chem.*, 1979, **18**, 3015 and refs. therein.
2 O. Kahn, in 'Magneto-Structural Correlation in Exchange Coupled Systems,' eds. R. D. Willett, D. Gatteschi, and O. Kahn, D. Reidel, Dordrecht, 1984, p. 57.
3 D. N. Hendrickson, in ref. 2, p. 523.
4 J. A. C. Van Ooijen, J. Reedijk, and A. L. Spek, *Inorg. Chem.*, 1979, **18**, 1184.
5 M. Habenschuss and B. G. Gerstein, *J. Chem. Phys.*, 1974, **61**, 852.
6 O. Simonsen and H. Toftlund, *Inorg. Chem.*, 1981, **20**, 4044.
7 J-C. Trombe, A. Gleizes, and J. Galy, *C.R. Acad. Sci. Paris*, 1986, **302**, 21.
8 G. Bernardinelli, P. Castan, and R. Soules, *Inorg. Chim. Acta*, 1986, **120**, 205.
9 T. R. Felthouse, E. J. Laskowski, and D. N. Hendrickson, *Inorg. Chem.*, 1977, **16**, 1077; C. G. Pierpont, L. C. Francesconi, and D. N. Hendrickson, *ibid.*, 1978, **17**, 3470.
10 D. Coucouvanis, D. G. Holah, and F. J. Hollander, *Inorg. Chem.*, 1975, **14**, 2657.
11 J. J. Bonnet, P. Cassoux, P. Castan, J. P. Laurent, and R. Soules, *Mol. Cryst. Liq. Cryst.*, 1987, **142**, 113.
12 A. Mosset, J-J. Bonnet, and J. Galy, *Acta Crystallogr., Sect. B*, 1977, **33**, 2639.
13 B. A. Frentz, SDP Structure Determination Package, Enraf-Nonius, Delft, Holland, 1982.
14 P. Coppens, L. Leiserowitz, and D. Rabinovitch, *Acta Crystallogr.*, 1965, **18**, 1035.
15 G. M. Sheldrick, SHELX 76, Program for *X*-Ray Crystal Structure Determination, University of Cambridge, 1976.
16 'International Tables for *X*-Ray Crystallography,' eds. J. A. Ibers and W. C. Hamilton, Kynoch Press, Birmingham, 1974, vol. 4.
17 D. Semmingen, *Acta Chem. Scand.*, 1973, **27**, 3961; D. Semmingen, F. J. Hollander, and T. F. Koetzle, *J. Chem. Phys.*, 1977, **66**, 4405.
18 L. J. Bellamy and A. J. Owen, *Spectrochim. Acta, Part A*, 1969, **25**, 329.
19 P. M. Gidney, R. D. Gillard, and B. T. Heaton, *J. Chem. Soc., Dalton Trans.*, 1973, 132.
20 A. Meyer, A. Gleizes, J-J. Girerd, M. Verdaguer, and O. Kahn, *Inorg. Chem.*, 1982, **21**, 1729.
21 C. Y. Weng, Ph.D. Thesis, Carnegie Institute of Technology, 1968.
22 W. E. Ester, R. R. Weller, and W. E. Hatfield, *Inorg. Chem.*, 1980, **19**, 26.
23 B. N. Figgis, *Trans. Faraday Soc.*, 1960, **56**, 1553.
24 R. L. Carlin, *J. Chem. Educ.*, 1966, **10**, 521.

Received 31*st December* 1986; *Paper* 6/2491